# Purge Dynamics of Fuel Cells

**DIMITRI GIDASPOW and SARVAJIT SAREEN**
*Institute of Gas Technology, Chicago, Illinois*

**An anisotropic porous media model has been suggested for fluid motion in fuel cell cavities and has been shown to be valid experimentally with an actual fuel cell plate. Analytical solutions for pressure, velocity, and stream function have been obtained for finite and for point sources and sinks in rectangular cavities. Constant purge time curves have been constructed.**

Fuel cell gas compartments are of two types: through-flow and dead-ended. Dead-ended anode and cathode compartments are used when pure reactants are available, such as hydrogen and oxygen in space vehicles. But even ultrapure fuels and oxidants have some impurities which accumulate and cause a drop in voltage due to the dilution of the reactants. Thus periodic purging is required. Purging must be accomplished with a minimum disturbance to the system. For example, in the case of the hydrogen-oxygen fuel cells with an aqueous electrolyte, fed with dry gases from cryogenic storage, a sharp increase of flow during the purge period over that of normal operation causes a loss of water with a drying out that may be reflected in slow voltage recovery or in permanent damage. The response of at least some of these cells (*1, 2*) to step changes in humidity is known to be very slow. Thus purging is done with inlet flows of not more than several times the stoichiometric consumption under load. Furthermore, purging should be accomplished with the least possible loss of reactants.

We see that the flow rate in such cells under normal operation and during purge is very low. In turn the pressure drop across these cells is very small. A small obstruction such as a water droplet at inlet may block the reactants from entering the cell, unless the inlet port is so small that the velocities are very high. Thus to insure that each cell in a battery connected to a common manifold is supplied with fresh reactant, the inlet ports are made very small to take the drop in pressure. This fact and constructional simplicity lead to the two-dimensional distribution of the reactants in the gas compartments. To solve such a two-dimensional problem, we must study the fluid mechanics in the cavity. The flow would be simply creeping motion between parallel plates were it possible to have empty cavities. However, structural rigidity and the desirability to have current collectors contacting the electrodes uniformly apparently led Allis-Chalmers (*3*) to build the gas compartments, called plates, with a complex internal geometry. Figure 1 shows the web type of structure of the gas compartments.

It appears that for rational design and improvement of dead-ended and nearly dead-ended fuel cells, one must have a good mathematical description of flow in the anode and cathode cavities. Such a model is needed in order to understand and optimize purging of accumulated inerts, to improve the web structure so as to minimize or eliminate inerts left behind after a purge with a minimum loss of reactants, to study the buildup of inerts during normal operation without the necessity of assuming the flow to be one dimensional, and to understand the water balance problem and the related loss of electrolyte, again without making a one-dimensional assumption. The one-dimensionality assumption is immediately suspect owing to the facts that the cell is nearly square and the inlet and exit ports are pin holes.

The web structure of the cavities is geometrically so complicated that an exact analysis based on the Navier-Stokes equations appeared to be at first out of the question. It turns out, however, that the rates of flow even during purge are sufficiently low and the surface area due to narrow passages is sufficiently high for the flow to be in the shear regime. We know that at Reynolds numbers less than one flow between parallel plates is in the Hele-Shaw regime (*4*). The pressure satisfies Laplace's equation. Analogously, flow in porous media follows Darcy's law for Reynolds numbers less than 10 (*5*). In porous media, however, the constant of proportionality between velocity and pressure drop cannot be accurately related to the geometry of the porous medium structure. It is determined empirically (*6*). Owing to the complexity of the geometry of the web structure, we also decided to obtain this parameter empirically. For the case of uniform passages in the two directions, it is only necessary to know the ratio of the permeabilities. This paper is the first attempt at a mathematical description of the purge problem.

## POROUS FLOW MODEL

As already stated owing to the geometrical complexity of the fuel cell cavities and the low flow and the high surface area contacting the fluid, it appears reasonable to approximate the fluid mechanics by use of Darcy's law. The permeability may be taken to be a function of position and is allowed to have different values in different directions. In addition, the depth of the gas compart-

ments is so small that we can work with some depth averaged velocities. We are primarily interested in the flow distribution in two directions. The permeabilities to be determined experimentally will properly reflect the averaging process. In both the hydrogen and the oxygen compartments, the reactants are consumed at one wall, and in the hydrogen chamber, the water produced is removed at the other wall. Thus in the two-dimensional mass balance given below, a sink is added in the differential equation. The mass balance becomes

$$\frac{d}{dt}\iiint \epsilon\rho\, dV + \oiint \rho\vec{v}_s dS = -\iint \text{sink} \cdot dS_w \quad (1)$$

where sink represents the rate of mass consumption per unit wall area.

Applying the divergence theorem and shrinking the volume element, we get the differential equation below

$$\epsilon\frac{\partial\rho}{\partial t} + \nabla\cdot\rho\vec{v}_s = -\text{sink}\cdot\frac{S}{V} \quad (2)$$

The differential form of Darcy's law with zero gravity is

$$\vec{v} = \frac{\vec{v}_s}{\epsilon} = -\frac{k}{\mu}\nabla P \quad (3)$$

The permeability used here equals that used in Scheidegger divided by the porosity, for example, see Scheidegger's equation 6.2.2.6 (6). This was done for easy reduction to flow in an equivalent empty cavity.

Owing to small density changes, consider $\rho$ and $P$ to be equal to some constant values plus perturbation values. Then substitution of Equation (3) into the continuity equation and the neglect of second-order infinitesimals yields

$$\frac{\mu}{\rho}\frac{\partial\rho}{\partial t} = \frac{\partial}{\partial x_A}\left(k_x\frac{\partial P}{\partial x_A}\right) + \frac{\partial}{\partial y_A}\left(k_y\frac{\partial P}{\partial y_A}\right) - \text{sink}\cdot\frac{S}{V\epsilon}\frac{\mu}{\rho} \quad (4)$$

where $k = k(x_A, y_A)$ in general, and $x_A$ and $y_A$ are the actual coordinates. Initially the effect of compressibility $\partial\rho/\partial t$ and the sink will be neglected.

The neglect of the compressibility effect is not unreasonable owing to the small pressure changes and is necessary in modeling for the sake of generality. Similarly, since the mass consumption by the electrochemical reaction changes in as yet some unknown fashion during purge, its effect is ignored. The Green's function technique used in this paper, however, allows one to easily include the effect of consumption. A preliminary estimate has shown that the addition of a constant sink uniformly distributed throughout the cell does not alter the conclusions reached in this study. Although a stream function no longer exists, the pressure and the velocity curves caused by such a sink are similar to those presented here. Also the steady state solution of the nonlinear pressure equation with a variable density can be reduced to the problem of the solution of the Laplace's equation solved here by making a change of the dependent variable, as discussed by Scheidegger (6).

## PRESSURE, VELOCITY, AND STREAM FUNCTION

For constant permeabilities in the $x$ and $y$ directions, Equation (4) becomes

$$\frac{\mu}{\rho}\frac{M}{g_cRT}\frac{\partial P}{\partial t} = k_x\frac{\partial^2 P}{\partial {x^2}_A} + k_y\frac{\partial^2 P}{\partial {y^2}_A} \quad (5)$$

by using the ideal gas law. The internal geometry of the hydrogen chambers is such that if we relate the permeabilities to an effective radius based on open area, it becomes reasonable to assume $k_x$ and $k_y$ to be constant but different in different directions (see Figure 1.) Comparison of Darcy's law with the Hagen-Poiseuille equation for a tube shows that the permeability equals $\frac{1}{8}\, r^2$, where $r$ is the tube radius (6). The present oxygen chamber is only slightly more complex geometrically. For a nearly constant density $\rho$, the partial differential equation is linear, and its solution can be readily obtained by the method of Green's functions for either finite inlet and exit ports or for point sources and sinks. The linearity is due to the fact that the pressure during the purge period deviates only slightly from the normal operating pressure. The pressure in Equation (5) can thus be viewed as a

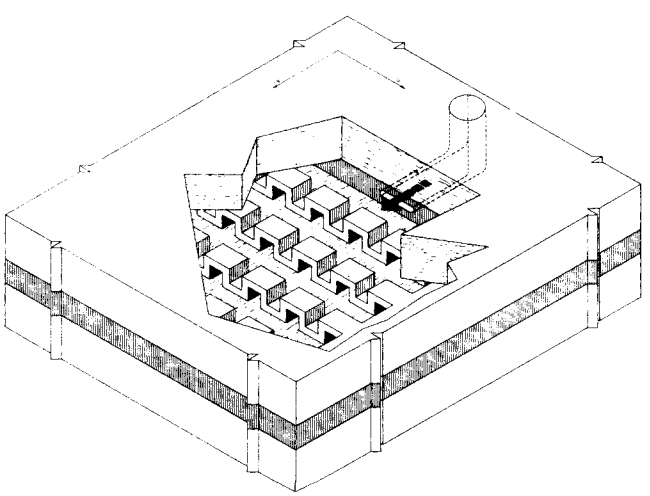

Fig. 1. Web structure of a fuel cell plate.

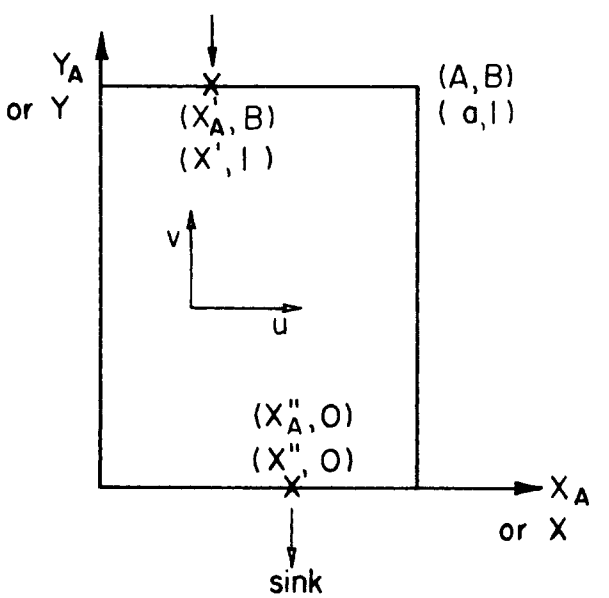


Fig. 2. Coordinates for flow.

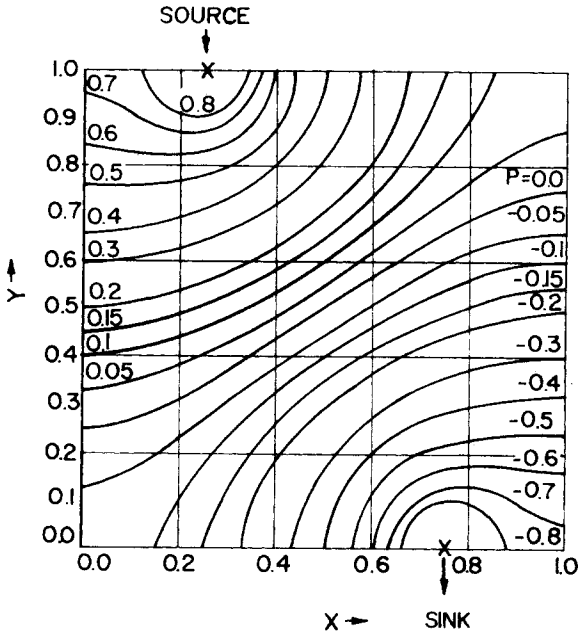


Fig. 3. Isobars for the case of a square plate with $a = 1$.

perturbation pressure.

Consider a rectangle $0 < x_A < A$, $0 < y_A < B$. The fluid enters the region at $(x'_A,B)$ and leaves at $(x''_A,0)$ (see Figure 2). The normal derivative of pressure is zero at all boundaries, except at the source and at the sink. The necessary condition for the existence of the steady Neumann problem is that the line integral of the normal derivative be zero around the closed boundary of the region. This merely requires that the inlet rate of flow be equal to the exit flow. If we specify the flow, as we must with a point source, the pressure in the cavity will be known if we know the pressure at one point.

In the two-dimensional continuum model used, the average velocity in the $y_A$ direction defined as

$$\frac{1}{A}\int_0^A v\,dx_A \tag{6}$$

is a constant, since all the flow passes between the two boundaries of the rectangle. We equate this to the average velocity calculated from the input which is $BQ/V_g$. In passing we observe that $V_g/Q$ is a residence time. The material balance thus becomes

$$\frac{QAB}{V_g} = \int_0^A -v\,dx_A \tag{7}$$

If we apply Equation (7) at the inlet boundary, the integration extends over the width of the hole only. Then as the hole becomes smaller and smaller, the velocity through the hole must become larger and larger to give a nonzero input. Since the velocity equals a constant times the pressure gradient, it is clear that the pressure gradient must also go to infinity as the port size approaches zero.

To reduce the number of parameters in the physical problem described, we introduce the following scale factors. We use the actual length of the rectangle $B$ as the scale factor for distance. Let

$$y = y_A/B \tag{8}$$

Then the partial differential equation for pressure, Equation (5), shows that the other distance coordinate and time must be scaled as shown below for the coefficients in the differential equation to equal unity:

$$x = (x_A/B)\sqrt{k_y/k_x} \tag{9}$$

$$\tau = \frac{\rho g_c RT\,k_y\,t}{\mu MB^2} \tag{10}$$

The rectangle $A \times B$ transforms into $a \times 1$, where

$$a = (A/B)\sqrt{k_y/k_x} \tag{11}$$

The source condition, Equation (7), gives us a unit strength of source if we let

$$\bar{v} = (v\,V_g)/(QA\sqrt{k_y/k_x}) \tag{12}$$

By using

$$v = -(k_y g_c/\mu)\frac{\partial P}{\partial y_A} \tag{13}$$

define the dimensionless pressure $\bar{P}$ as

$$\bar{P} = \frac{(V_g\sqrt{k_y k_x})P}{QAB\mu/g_c} \tag{14}$$

Then we have for a unit source

$$1 = \int_0^a -\bar{v}\,dx = \int_0^a \frac{\partial \bar{P}}{\partial y}\,dx \tag{15}$$

and for the differential equation for pressure

$$\frac{\partial \bar{P}}{\partial \tau} = \frac{\partial^2 \bar{P}}{\partial x^2} + \frac{\partial^2 \bar{P}}{\partial y^2} \tag{16}$$

with

$$\bar{v} = -\frac{\partial \bar{P}}{\partial y} \text{ and } \bar{u} = -\frac{\partial \bar{P}}{\partial x} \tag{17}$$

where the velocity component $\bar{u}$ has been scaled in a natural way as

$$\bar{u} = (u\,V_g)/QA \tag{18}$$

For the usual purge times of interest, the dimensionless time $\tau$ is a very large number. For example, for a purge time of 6 sec., $\tau$ is of the order of $10^4$. Owing to this fact,

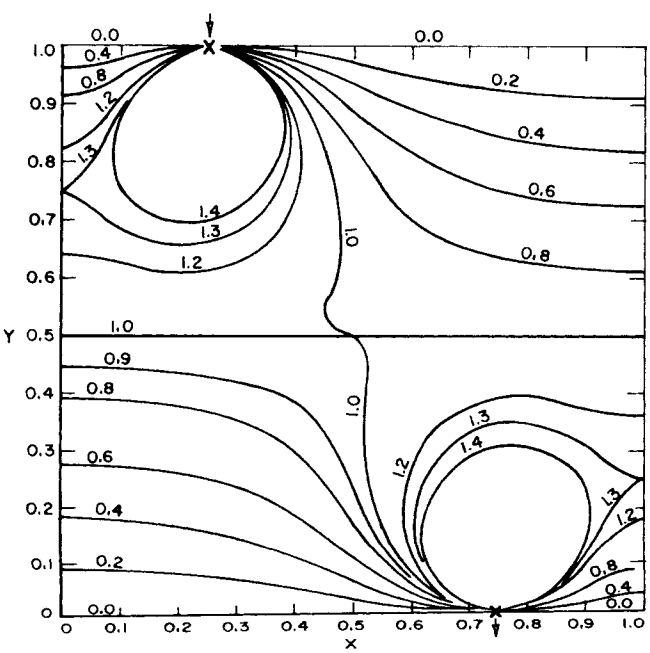


Fig. 4. Velocity component $\bar{v}$ for a square plate with $a = 1$.

only steady state solutions are of interest. This is clear from both the analytical solutions to the diffusion equation and from simple dimensional analysis of Equation (16). If we scale the real time with purge time, the coefficient of the partial of pressure with respect to time becomes very small compared with one. This shows that we can set this partial derivative equal to zero. The pressure and velocity are now a function of three parameters $x$, $y$, and $a$, in addition to the location of the source and sink.

The solution to the unit source-sink problem for the Laplace's equation will be obtained as the limit of the unsteady two-dimensional Equation (16) by using the method of Green's functions. To completely define the unsteady problem, we must specify the initial distribution. We choose it to be zero, for convenience, since we are interested in the steady problem anyway. The Green's function for the two-dimensional diffusion equation with zero gradient at the boundaries is given in Carslaw and Jaeger (7) by Equation 14.4-(4). The time-dependent pressure distribution with an instantaneous unit point source at $(x', 1)$ and a unit instantaneous point sink at $(x'', 0)$ is simply the difference between the Green's functions evaluated at $(x', 1)$ and at $(x'', 0)$, respectively. The time dependent distribution due to sources and sinks up to time $\tau$ is simply the integral of the expressions from zero to $\tau$. To obtain the pressure due to a continuous unit source and sink, we let time $\tau$ go to infinity. Thus the pressure distribution with a point source at $(x', 1)$ and a point sink at $(x'', 0)$ is given by the following expression:

$$\bar{P} = \frac{2a}{\pi^2}\sum_{n=1}^{\infty}\frac{1}{n^2}\left(\cos\frac{n\pi x'}{a} - \cos\frac{n\pi x''}{a}\right)\cos\frac{n\pi x}{a} + \frac{2}{a\pi^2}\sum_{m=1}^{\infty}\frac{1}{m^2}\left[(-1)^m - 1\right]\cos m\pi y + 4a\sum_{n=1}^{\infty}\sum_{m=1}^{\infty}\frac{1}{n^2\pi^2 + a^2m^2\pi^2}\left[(-1)^m\cos\frac{n\pi x'}{a} - \cos\frac{n\pi x''}{a}\right]\cos\frac{n\pi x}{a}\cos m\pi y \qquad (19)$$

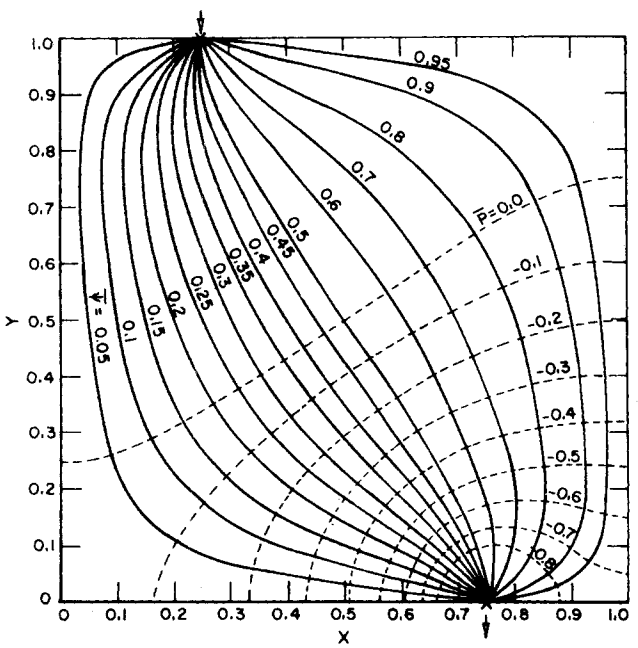


Fig. 5. Stream function for a square plate with $a = 1$.

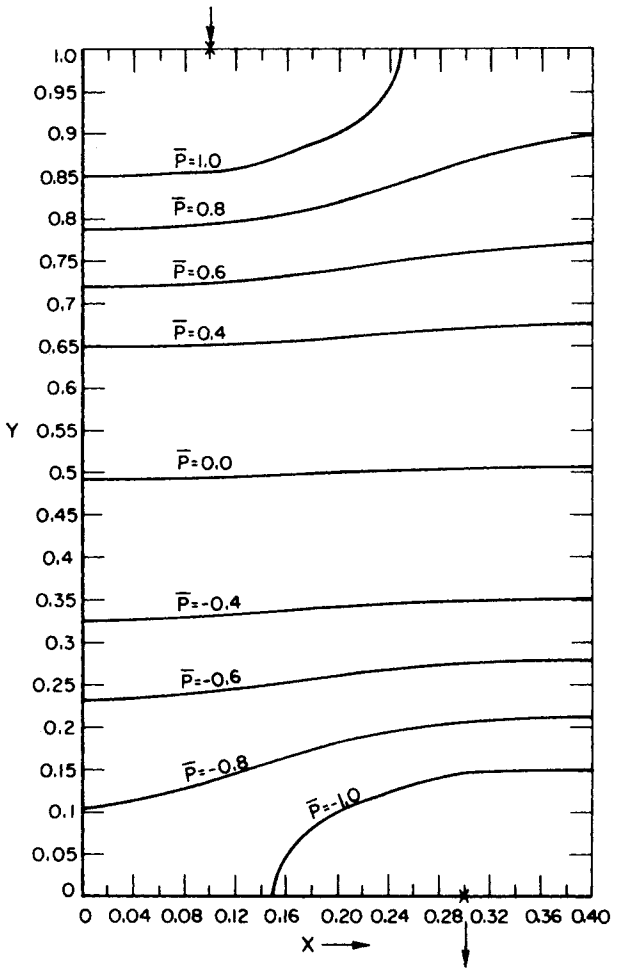


Fig. 6. Isobars for the case of $a = 0.4$ ($k_x/k_y = 2.2$ and $A/B = 0.6$).

The velocity components $\bar{u}$ and $\bar{v}$ may be obtained by differentiating the expression for pressure with respect to $x$ and $y$, respectively. This differentiation yields

$$\bar{u} = -\frac{2}{\pi}\sum_{n=1}^{\infty}\frac{\sin\frac{n\pi x}{a}}{n}\left(\cos\frac{n\pi x'}{a} - \cos\frac{n\pi x''}{a}\right) - \frac{4}{\pi}\sum_{n=1}^{\infty}\sum_{m=1}^{\infty}\frac{n\left(\sin\frac{n\pi x}{a}\cos m\pi y\right)}{n^2 + a^2m^2}\left[(-1)^m\cos\frac{n\pi x'}{a} - \cos\frac{n\pi x''}{a}\right] \qquad (20)$$

and

$$\bar{v} = \frac{4}{a\pi}\sum_{m=1}^{\infty}\frac{\sin(2m-1)\pi y}{(2m-1)} - \frac{4a}{\pi}\sum_{n=1}^{\infty}\sum_{m=1}^{\infty}\frac{m\left(\cos\frac{n\pi x}{a}\sin m\pi y\right)}{n^2 + a^2m^2}\left[(-1)^m\cos\frac{n\pi x'}{a} - \cos\frac{n\pi x''}{a}\right] \qquad (21)$$

The stream function $\psi$ is useful in visualizing the flow and in obtaining the purge times which are discussed in a later section.

By using the standard definition of the stream function, a dimensionless stream function may be defined for this problem as

$$\overline{\psi} = \frac{V_g}{QAB}\psi$$

Having derived an expression for the pressure potential, we can easily obtain an expression for its harmonic conjugate, the stream function, using the property of exact differentials (8). In proving the sufficiency condition, caution must be exercised in choosing the path of integration. If the expression is integrated with respect to $x$, then care must be taken not to integrate through the discontinuity (the source or sink) but around it. If the expression is integrated with respect to $y$, then we automatically avoid the discontinuities, except at $y = 0$ and $y = 1$, where the expression for the stream function gives $\overline{\psi} = 0$ because of the property of the Fourier series.

The final expression for the stream function is given by

$$\overline{\psi} = \frac{4x}{a\pi}\sum_{m=1}^{\infty}\frac{\sin(2m-1)\pi y}{(2m-1)} - \frac{4a^2}{\pi^2}\sum_{n=1}^{\infty}\sum_{m=1}^{\infty}\frac{m\left(\sin\frac{n\pi x}{a}\sin m\pi y\right)}{n(n^2+a^2m^2)}\left[(-1)^m\cos\frac{n\pi x'}{a} - \cos\frac{n\pi x''}{a}\right] \quad (22)$$

### Finite Inlet and Outlet Ports

Some fuel cells have finite inlet and exit ports. It is, therefore, useful to have an analytic solution to describe this physical situation.

The solution to the finite hole case may be obtained from the instantaneous point source solution by integrating the Green's function in Carslaw and Jaeger (7) over the size of the hole and then over the time interval. The steady state solution is obtained by letting the time go to infinity:

$$P' = \lim_{\tau\to\infty}\int_0^{\tau} d\tau'\left[\int_{x_1}^{x_2} G(x, y; x', 1, \tau-\tau')dx' - \int_{x_3}^{x_4} G(x, y; x', 0, \tau-\tau')dx'\right] \quad (23)$$

After integration and reduction to steady state, the pressure distribution assumes the form

$$P' = \frac{2\Delta x_h}{\pi^2 a}\sum_{m=1}^{\infty}\left[\frac{(-1)^m-1}{m^2}\right]\cos m\pi y + \frac{2a^2}{\pi^3}\sum_{n=1}^{\infty}\frac{1}{n^3}\cos\frac{n\pi x}{a}\left[\sin\frac{n\pi x_2}{a} + \sin\frac{n\pi x_3}{a} - \sin\frac{n\pi x_1}{a} - \sin\frac{n\pi x_4}{a}\right] + \frac{4}{\pi_3}\sum_{n=1}^{\infty}\sum_{m=1}^{\infty}\frac{1}{n}\frac{\cos m\pi y\cos n\pi x/a}{n^2/a^2+m^2}\left[(-1)^m\left(\sin\frac{n\pi x_2}{a} - \sin\frac{n\pi x_1}{a}\right) - \left(\sin\frac{n\pi x_4}{a} - \sin\frac{n\pi x_3}{a}\right)\right] \quad (24)$$

where

$$\Delta x_h = x_2 - x_1 = x_4 - x_3 \quad (25)$$

The source is located between $(x_2, 1)$ and $(x_1, 1)$. The sink is bounded by the coordinates $(x_4, 0)$ and $(x_3, 0)$.

Normalizing the pressure $P'$ yields the pressure for a unit source $\overline{P}$:

$$\overline{P} = \frac{P'}{\Delta x_h} \quad (26)$$

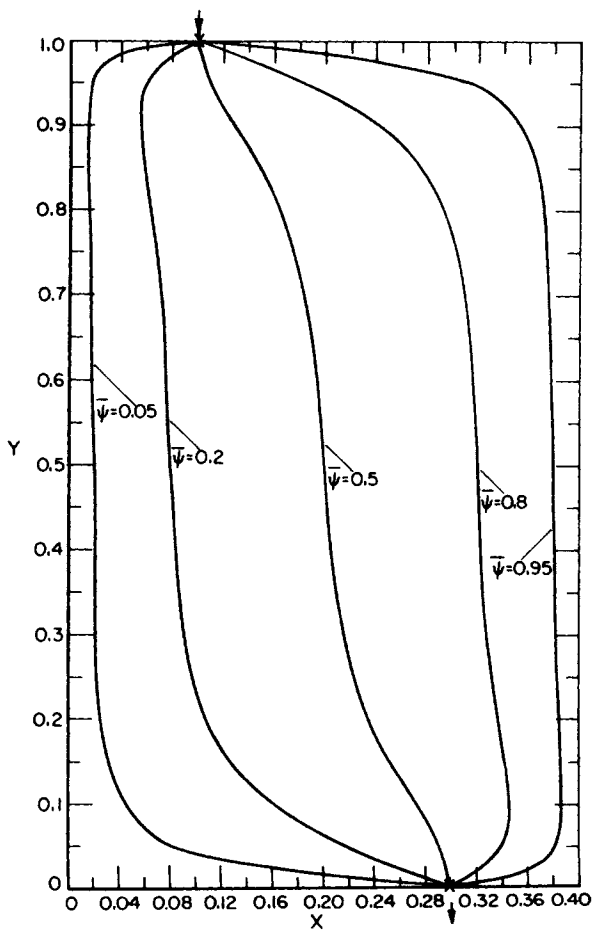


Fig. 7. Streamlines for the case of $a = 0.4$ ($k_x/k_y = 2.2$ and $A/B = 0.6$).

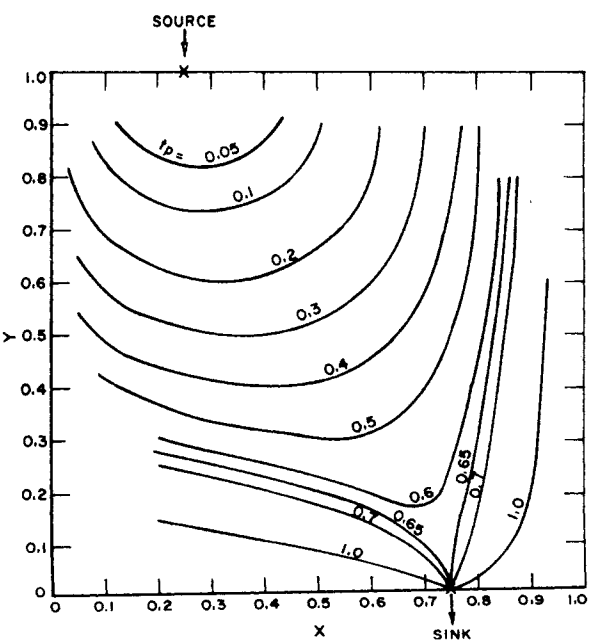


Fig. 8. Purge time curves for a square plate with $a = 1$.

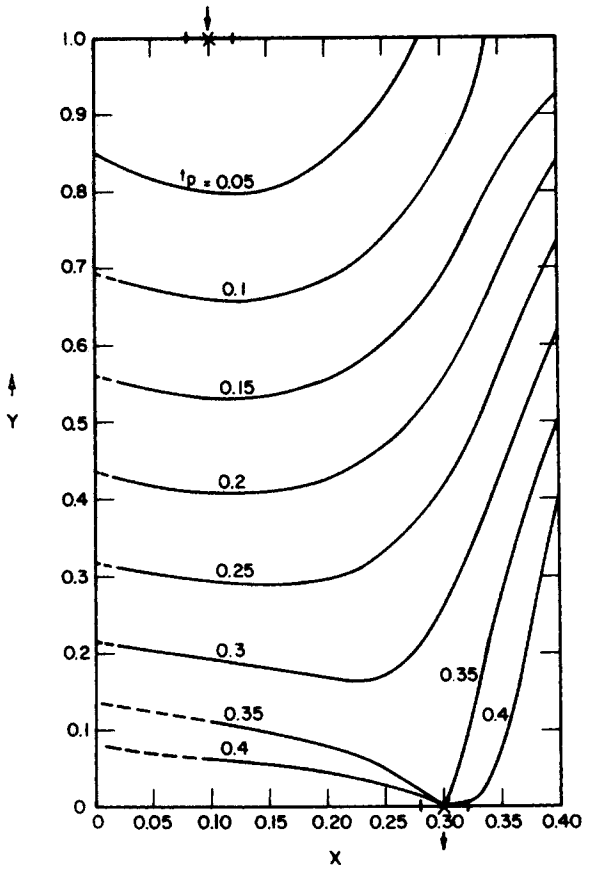


Fig. 9. Purge time curves for the case of $a = 0.4$ ($k_x/k_y = 2.2$ and $A/B = 0.6$).

The expressions for the pressure distribution, Equations (19) and (24), lend themselves easily to obtaining a distribution because of their rapid convergence. The expressions for the velocity components and the stream function, however, converge very slowly, and computation time becomes prohibitively long on a small computer.

Since, however, all the above expressions obey the rules for summability (*9, 10*), they were reduced to standard forms whose sums are readily available (*11, 12*).*

## NUMERICAL RESULTS

Three cases presented in this work are:

1. Square plate with a permeability ratio of 1, for the case of a point source and sink.
2. Rectangular plate whose aspect ratio is 0.6 and permeability ratio is 2.2, for the case of a point source and sink.
3. Square plate with a permeability ratio of 1, for the case of a finite hole size for the source and sink. The hole sizes were 13% of the width of the rectangle.

Pressure, the $\bar{v}$ component of velocity, and the stream function for case 1 are graphically represented in Figures 3 through 5. This case of $a = 1$ is a truly two-dimensional case, and an analysis of this situation permits an insight into the conditions of flow present in the plate. From Figure 3 we see that near the source and the sink the isobars are nearly perfect semicircles. This is a result of the easily verifiable fact that the lines of constant potential for a point source or sink in a half plane are semicircles, while the stream functions are rays (see Figure 5). The velocity component graphs, such as shown in Figure 4, illustrate the complex behavior but are not particularly helpful in interpretation.

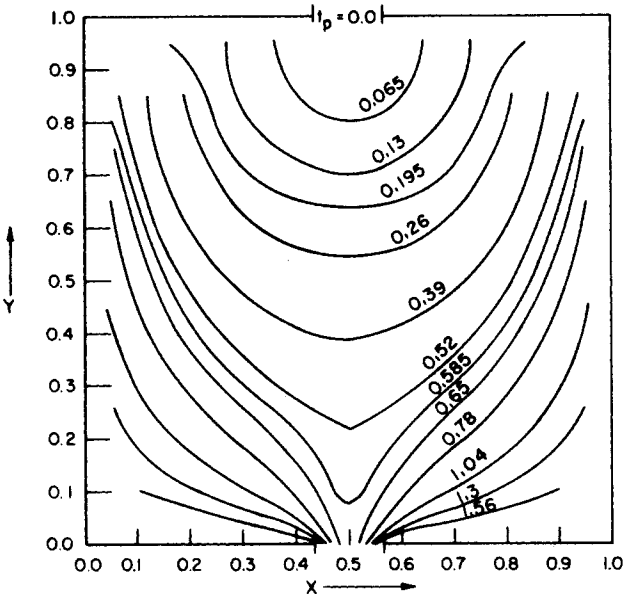


Fig. 10. Purge time curves for the case of finite size ports with $a = 1$.

For the cavity to be purged out uniformly requires that all the paths of flow be equal. An examination of Figure 5 reveals that for the case of "$a$" = 1 all the paths of flow are not the same. Therefore, for efficient purging of the cavity it is necessary to make the flow more unidirectional in the basic direction of flow; that is, $a$ must be less than one.

The plots for $a = 0.4$ (where $A/B = 0.6$ and $k_x/k_y = 2.2$) are presented in Figures 6 and 7. These values were chosen to illustrate an actual case of a fuel cell plate, with permeabilities estimated on the basis of area available for flow. Results for a smaller $a$ are shown later.

In this case, the fluid is almost immediately swept out in the $x$ direction and then moves uniformly as an entire mass in the $y$ direction. As a result of this, the paths of flow are almost the same (Figure 7), and the area of the plate swept is substantially different from the case of $a = 1$.

## PURGE TIMES

One of the objects of this study is to predict how many impurities stay in the cavity after a purge of a given duration. This information will help the design of a better cell. To some extent the answer to this problem depends upon the distribution of inerts just before purge. The initial distribution depends upon how and how long the cell was operated before purge. This introduces a number of additional parameters into the problem, and its solution depends upon the knowledge of the velocity distribution in the cavity under normal operation, which will be obtained with the help of this study. It is, however, possible to simplify the problem if we simply look at the discontinuity between the fresh fluid injected at purge and that present in the cell before the exit valve was opened. If we neglect molecular diffusion compared with bulk flow, this discontinuity will be sharp. The Allis-Chalmers group (*14*) carried out such a modeling study

* The summed material has been deposited as document 00929 with the ASIS National Auxiliary Publications Service, c/o CCM Information Sciences, Inc., 22 W. 34th St., New York 10001 and may be obtained for $2.00 for microfiche or $5.00 for photocopies.

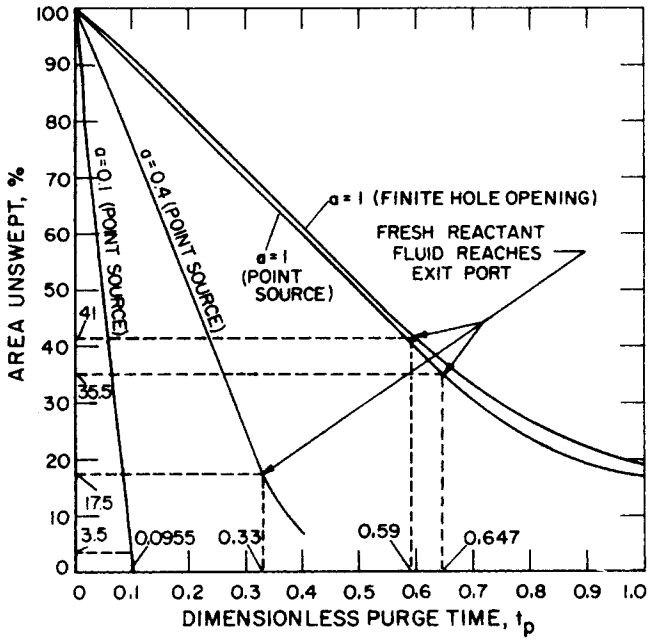


Fig. 11. Effect of plate geometry on purge efficiency.

not mathematically but by substituting water for the fuel cell gases. At zero time a colored dye was injected, and the moving front was photographed. Constant time lines were constructed for their basic plates and for modified plates.

By knowing the velocity components, the flow distribution experiments carried out at Allis-Chalmers (*14*) may be performed on a computer. If $C$ refers to the colored liquid injected, the differential equation without dispersion is, in dimensionless form

$$\frac{\partial C}{\partial t_p} + \bar{u}\frac{\partial C}{\partial x} + \bar{v}\frac{\partial C}{\partial y} = 0 \qquad (27)$$

By the theory of characteristics, we can write

$$\frac{dt_p}{1} = \frac{dx}{\bar{u}} = \frac{dy}{\bar{v}} = \frac{dC}{0} \qquad (28)$$

Equation (28) gives the position of the colored liquid injected as a function of time in terms of the velocity components $\bar{u}$ and $\bar{v}$.

The dimensionless purge time $t_p$ is related to the real purge time by

$$t_p = (Q/V_g)(A/B)\sqrt{k_y/k_x}\ (\text{real time}) \qquad (29)$$

The constant purge time lines were obtained from the following integrals of the diffusion equation without dispersion and were integrated along constant streamlines:

$$t_p = \int_{(x',1)}^{(x,y)} \frac{dx}{\bar{u}} = \int_{(x',1)}^{(x,y)} \frac{dy}{\bar{v}} \qquad (30)$$

To further clarify the procedure, we note that Equation (27) rewritten in Lagrangian form, that is following a particle, is simply

$$\frac{dC(t, x(t), y(t))}{dt} = 0 \qquad (31)$$

This characteristic form says that the particle at the discontinuity, that is, the front, travels unchanged with velocity components $\bar{u}$ and $\bar{v}$. But since in our case all the fluid particles also move along these paths, which are the streamlines, we see that the front also moves along these stream lines. When, however, we include consumption of fuel at the walls, then in the two-dimensional mass balance the divergence of velocity is not zero, and streamlines do not exist. Mathematically, in such a case, the line integral around a closed path is not zero. Therefore, the line integral does not define a function. Physically, we can follow a particle until it is consumed at the wall and leaves the system. In such a situation we must find the purge times in a different way. We can simply move in the $y$ direction from the inlet using the $v$ component of velocity and then move in the $x$ direction using the $u$ component to any desired point. Several values of purge time were calculated by using this method. All other purge times were obtained by using the simpler procedure of integrating along the streamlines in the results presented here.

Figures 8 through 10 show the purge time curves for the three cases discussed in the section on numerical results. Figure 8 shows that for the case of equal permeabilities, the constant time curves are semicircles near the source. It is easy to show that the constant time curves for the case of a point source in a half plane are indeed semicircles. Equation (27) with radial symmetry becomes

$$\frac{\partial C}{\partial t_p} + v_r\frac{\partial C}{\partial r} = 0 \qquad (32)$$

Equation (32) gives the elementary fact that

$$\frac{dr}{dt_p} = v_r \qquad (33)$$

where $v_r$ is inversely proportional to the radius $r$. Thus, integration of Equation (33) shows that $t_p$ = constant curves are circles with the origin at the source. The constant pressure curves were circles for both the source and the sink. From Figure 8 we see that the constant time curves near the sink are, as expected, not circles but narrow down to a corner as the fresh fluid tries to escape through the outlet hole. Figure 10 shows that the finite opening case does not produce marked differences. Near the sink the narrowing is not as sharp, but the time the fresh fluid first reaches the exit port was not decreased significantly. Figure 9 shows that with a lower permeability in the direction of flow, the constant purge time

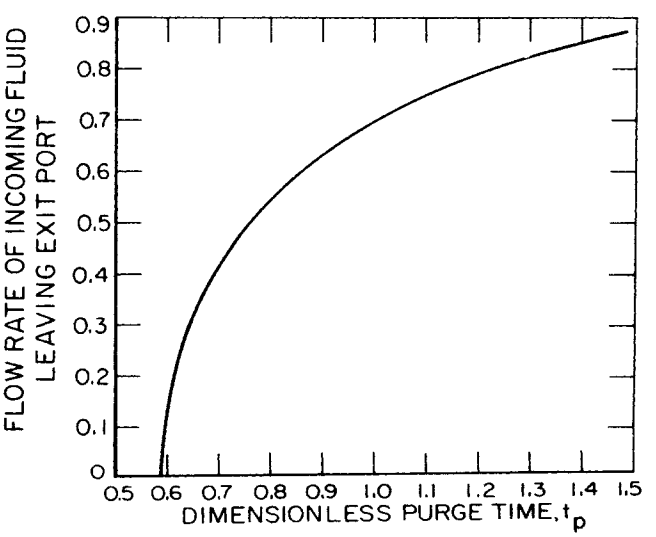


Fig. 12. Loss of reactant fluid during purge for the case of finite size ports with $a = 1$.

curves near the source tend to be elliptical, as is expected.

At the time when the first fluid reaches the exit port Figure 11 shows that the difference between the two cases for $a = 1$ is only 6% in the area swept. This difference arises from the different positions of the source-sink coordinates. The difference between the case for $a = 1$ and $a = 0.4$, Figures 8 and 9, shows a substantial improvement, 18%. The reason for this lies in the increased permeability in the $x$ direction and the reduction of a square plate to a rectangle. Both of these factors cause the flow to be more unidirectional in the basic direction of flow.

Figure 11 also shows the area unswept for the case of $a = 0.1$. At this value of $a$ the amount of cavity left unswept, at the time when the first fluid reaches the exit port, is 3.5%. It is interesting to note that the area unswept — purge time relationship is almost linear for this value of $a$. For an aspect ratio $A/B$ of 0.6, the permeability ratio $k_x/k_y$ is 36 in this case.

The point when the fresh incoming fluid first reaches the exit port is important, because after that fresh reactant is being thrown out. Had the cell been full of inerts before the purge was started, we would not wish to stop the purge sooner, because until that time only inerts were being thrown out. Had the cell been only partially filled with inerts, it would be wasteful to continue purging much beyond that point, especially since during operation of the fuel cell the inerts accumulate in the cavity away from the source. Figure 10, for example, shows that after a dimensionless purge time of 0.594, fresh reactant fluid along with the fluid previously contained in the compartment is being purged. Figure 12 shows the flow of incoming fluid leaving the exit port as a function of purge time. It can be used to determine current loss due to reactant wastage, given an initial concentration in the cell before purge. Although an optimum purge time will depend upon the initial distribution of inerts before the purge, based on simplified models (*15*) we determined that one would not want to continue purging much beyond the time when the fresh fluid reaches the exit port.

## EXPERIMENT

The entire analysis and the model for purging is based on the assumption of low Reynolds number flow and on the applicability of Darcy's law. Therefore it becomes necessary to be able to verify this assumption. To do this an experiment was set up whose layout is shown in Figure 13. The plate used was the one supplied by Allis-Chalmers, and pressure drops across the plate were measured for various flow rates. The experiment was conducted with air at a pressure of 30 lb./sq.in.gauge and at room temperature. The fuel cell plate was clamped between two ½-in. plexiglass plates and sealed from leaks with RTV and high vacuum silicon. Two taps of 1/64-in. diameter were drilled to contact the second groove from each end of the plate to which pressure leads were attached. The distance between the taps was 0.52 ft. The pressure differential was measured with the aid of an MKS-Baratron pressure sensor unit, whose maximum operable range is 0 to 1 mm. Hg. The lowest value this unit can read is $3 \times 10^{-4}$ mm. Hg., and this is further divided into thirty parts. The flow was controlled accurately with a flow controller. The flow controller was placed after the plate so that the entire pressure drop took place through a needle valve. Sonic flow through the outlet valve prevented the propagation of fluctuations of ambient pressure into the cavity. Until this was done, it was not possible to measure the small drop in pressure. The rotameter was calibrated with the help of a bubble meter.

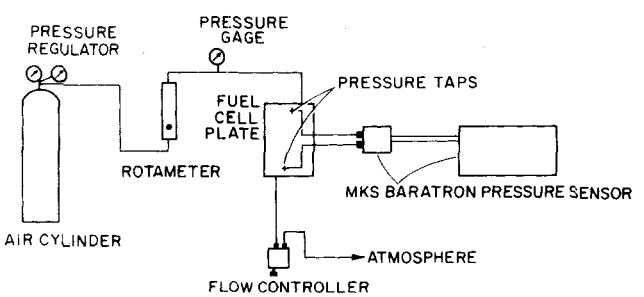


**Fig. 13. Experimental layout.**

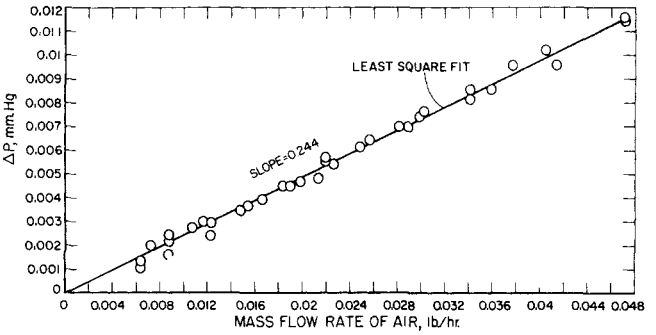


**Fig. 14. Verification of Darcy's law for an actual fuel cell plate.**

The results of the mass flow rate vs. pressure drop study are plotted in Figure 14. A straight line through the points was fitted by using the method of least squares. This experiment shows that for the flow rate range considered, the relationship between flow and pressure is indeed linear, as is assumed in the model. When air is used to simulate the conditions in the oxygen and hydrogen plates generating 150 ma./sq.cm. (*13, 14*), it is found that the flow rates required for this current generation lie well within the range covered in the experiment.

The measurement permits us to obtain a good approximation to the permeability in the $y$ direction. Equation (7) together with Darcy's law gives

$$\int_0^A \frac{\partial P}{\partial y_A}\, dx_A = (\mu Q A B)/(k_y V_g) \qquad (34)$$

Equation (34) shows that the pressure drop in the $y$ direction should be independent of $y_A$ and that there exists a mean value of $x_A$ at which we can obtain the true permeability $k_y$ from one pressure drop measurement. To obtain this correct mean value of position, we need to know the complete distribution. However, since the geometry of the plate indicates that by far the largest drop of pressure is in the $y$ direction, the measured value of the pressure drop gives an approximation to the permeability $k_y$.

This calculated permeability for the oxygen fuel cell plate is $3.12 \times 10^{-7} \pm 4 \times 10^{-9}$ sq.ft. Using the formula

$$k_y = h^2/12 \qquad (35)$$

we can estimate the equivalent distance between parallel plates for this geometry. This depth $h$ is 0.0232 in. This is only a little lower than the actual height of the groove in the ribs of the oxygen plate which is 0.025 in. The experimental value must be lower, because the resistance through the groove is not the complete resistance to flow. This comparison is made on the assumption that the groove is very wide compared with its depth. Since the width is 0.078 vs. 0.025 in. for the depth, the other two walls have obviously some effect. An equivalent radius calculated from the pressure drop measurement gives a value of 0.019 in.

which, as expected, is lower yet than the geometrical equivalent value.

## RECOMMENDATIONS

It appears reasonable to improve the web structure by increasing the number of slots in the ribs running across the plate, keeping the flow area the same. This will increase the surface area-to-flow area ratio decreasing the permeability in the direction of basic flow. Its effect will be to make the flow more one dimensional and thus decrease the percent impurities unswept during purge.

Equation (11) shows that a decrease in the permeability ratio $k_y/k_x$ has the same effect as a decrease in the ratio of width-to-length. Purge time curves show the decrease of impurities left behind with a decrease in the effective aspect ratio $a$ as given by Equation (11). The position of ports, shape of the plate, and number of sinks are other parameters that may be varied to achieve a complete purge.


## ACKNOWLEDGMENT

This study was supported by the National Aeronautics and Space Administration under Contract No. NAS8-21159. The authors are very grateful to Richard Boehme of the NASA Marshall Space Flight Center for suggesting this practical problem. They also thank B. S. Baker, John Morgan, R. E. Peck, and C. W. Solbrig for a useful discussion of various aspects of the analysis.


## NOTATION

$a$ = dimensionless width of plate, $A/B\ \sqrt{k_y/k_x}$
$A$ = width of the plate, ft.
$B$ = length of the plate, ft.
$C$ = dimensionless concentration, $C'/C_{initial}$
$g_c$ = conversion factor, 32.2 $(lb._m)/(lb._f)$ (ft.)/(sec.$^2$)
$G$ = Green's function given by Equation 14.4-(4) in Carslaw and Jaeger
$h$ = distance between two parallel plates
$k$ = diagonal permeability matrix, sq. ft.
$k_x,k_y$ = permeabilities in the $x_A$ and $y_A$ directions, sq. ft.
$M$ = molecular weight, $lb._m$/(lb.) (mole)
$P$ = pressure, $lb._f$/sq. ft.
$\overline{P}$ = dimensionless pressure for unit input, $\dfrac{(V_g\sqrt{k_xk_y})P\ g_c}{QAB\mu}$
$P'$ = dimensionless pressure defined by Equation (23)
$Q$ = volumetric flow rate, cu. ft./sec.
$r$ = tube radius, ft.; radial coordinate as defined in Equation (33)
$R$ = universal gas constant, (ft.) $(lb._f)$/(lb.) (mole) (°R)
$S$ = surface, sq. ft.
$t$ = time, sec.
$t_p$ = dimensionless purge time, $\left(\dfrac{Q}{V_g}\right)\left(\dfrac{A}{B}\right)\left(\sqrt{\dfrac{k_y}{k_x}}\right)$ (real time)
$T$ = temperature, °R.
$u$ = velocity component in the $x_A$ direction, ft./sec.
$\overline{u}$ = dimensionless velocity in the $x$ direction, $\dfrac{V_g\,u}{QA}$
$v$ = velocity component in the $y_A$ direction, ft./sec.
$v_r$ = radial velocity component
$\overline{v}$ = dimensionless velocity in the $y$ direction, $\left(\dfrac{V_g}{QA}\sqrt{\dfrac{k_x}{k_y}}\right)v$
$\vec{v}$ = velocity vector, ft./sec.
$\vec{v}_s$ = superficial (filter) velocity vector, ft./sec.
$V$ = volume, cu. ft.
$V_g$ = volume of fluid in gas compartment, cu. ft.
$x$ = dimensionless space coordinate, $x_A/B\ \sqrt{k_y/k_x}$
$x_A$ = actual space coordinate, ft.
$x'$ = position of the source on the $x$ coordinate, dimensionless, $x_A'/B\ \sqrt{k_y/k_x}$
$x''$ = position of the sink on the $x$ coordinate, dimensionless, $x_A''/B\ \sqrt{k_y/k_x}$
$x_1,x_2$ = positions of the finite hole for the source on the $x$ coordinate, dimensionless, $x_{A1}/B\ \sqrt{k_y/k_x}$ and $x_{A2}/B\ \sqrt{k_y/k_x}$, respectively
$x_3,x_4$ = positions of the finite hole for the sink on the $x$ coordinate, dimensionless, $x_{A3}/B\ \sqrt{k_y/k_x}$ and $x_{A4}/B\ \sqrt{k_y/k_x}$, respectively
$y$ = dimensionless space coordinate, $y_A/B$
$y_A$ = actual space coordinate, ft.

### Greek Letters

$\Delta x_h$ = size of the port openings as defined by Equation (25), dimensionless
$\epsilon$ = porosity, volume void/total volume
$\mu$ = viscosity, $lb._m$/(ft.) (sec.)
$\rho$ = density $lb._m$ /cu. ft.
$\psi$ = stream function, sq. ft./sec.
$\overline{\psi}$ = dimensionless stream function, $\dfrac{V_g}{QAB}\psi$
$\tau$ = dimensionless time, $\dfrac{\rho g_c\,RT\,k_y}{\mu\,MB^2}\,t$

## LITERATURE CITED


1. Prokopius, P. R., and H. H. Hagedorn, *NASA TN D-4201* (1967).
2. Chase, C. A., Jr., Dimitri Gidaspow, and R. E. Peck, *Chem. Eng. Progr. Symposium Ser. No. 92*, **65**, 91-109 (1969).
3. Platner, J. L., and P. D. Hess, *Chem. Eng. Progr. Symposium Ser., No. 57*, **61**, 299-305 (1965).
4. Schlichting, H., "Boundary Layer Theory," 4 ed., McGraw-Hill, New York (1960).
5. Polubarinova-Kochina, P. Y., "Theory of Ground Water Movement," translated from Russian by J. M. Roger de Wiest, Princeton Univ. Press, N.J. (1962).
6. Scheidegger, A. E., "The Physics of Flow Through Porous Media," Univ. Toronto Press, Canada (1960).
7. Carslaw, H. S., and J. C. Jaeger, "Conduction of Heat in Solids," 2 ed., Oxford Univ. Press, New York (1959).
8. Streeter, V. L., "Fluid Dynamics," 1 ed., McGraw-Hill, New York (1948).
9. Knopp, K., "Theory and Application of Infinite Series," 2 ed., Blackie and Son, London, England (1966).
10. Goursat, E., and E. R. Hedrick, "A Course in Mathematical Analysis," Vol. 1, Dover Publications, New York (1959).
11. Jolley, L. B. W., "Summation of Series," 2 revised ed., Dover Publications, New York (1961).
12. Gradshteyn, I. S., and I. M. Ryzhik, "Tables of Integrals, Series and Products," 4 ed., Academic Press, New York (1965).
13. Allis-Chalmers, Research Division, *Contract No. NAS8-2696* for George C. Marshall Space Flight Center, NASA, Huntsville, Ala., Milwaukee, Wisc., (Sept. 30, 1965).
14. *Ibid.*, Sixth Quarterly Report (Dec., 31, 1965).
15. Institute of Gas Technology, *Contract No. NAS8-21159* for George C. Marshall Space Flight Center, NASA, Huntsville, Ala. Chicago, Ill. (Aug., 1968). (*NAS8-21159—SR—001*).



*Manuscript received October 8, 1968; revision received December 13, 1968; paper accepted December 16, 1968.*